Open camera or QR reader and
scan code to access this article
and other resources online.

Effect of Particle Size and Shape on Wall Slip of Highly Filled Powder Feedstocks for Material Extrusion and Powder Injection Molding

Daniel Sanetrnik,[1] Berenika Hausnerova,[1,2,i] Martin Novak,[1,2] and Bhimasena Nagaraj Mukund[2,3]

Abstract

A necessity to distinguish between the influence of powder shape and size (particle size distribution) is especially demanding for highly filled metal powder feedstocks employed in additive manufacturing and powder injection molding. As their processability is evaluated through rheological behavior, the study focuses on the effect of powder size/shape on a wall slip, which is a typical phenomenon determining flow performance of these materials. Water and gas atomized 17-4PH stainless steel powders with D_{50} of about 3 and 20 μm are admixed into a binder containing low-density polyethylene, ethylene vinyl acetate, and paraffin wax. Mooney analysis to intercept the slip velocity of 55 vol. % filled compounds reveals that wall slip effect appears to vary significantly with size and shape of metal powders—round shaped and large particles are the most prone to the wall slip. However, the evaluation is affected by the type of the flow streams resulting from the geometry of the dies—conical dies reduce the slip up to 60% in case of fine and round particles.

Keywords: material extrusion, powder injection molding, highly filled feedstock, wall slip, powder shape, particle size, die geometry

Introduction

ALTHOUGH ADDITIVE MANUFACTURING is merging with powder injection molding (PIM) in the field of production of highly precise metal items and gaining relevant attraction due to a combination of processability of plastics and mechanical, electric or magnetic properties of metals,[1] there are still fundamental issues not answered satisfactorily. An entire manufacturing process consists of four steps (mixing, material extrusion [MEX] additive manufacturing or PIM, debinding, and sintering) of an equal importance, which (if performed correctly) lead to the final metallic items of tight tolerances and high quality.[2] MEX and PIM have common three out of four steps; in case of MEX, there is an additional demand on sufficiently flexible filaments,[3–5] which however might be eliminated with extrusion designs based on granulate systems.[6,7]

Owing to the complexity of a multistep processing as MEX and PIM technology the current research is focused on the methods capable to intercept and reduce identified issues and defects prior sintering, that is, when the material can still be regranulated and reused.[8–10] One of the serious common complications is a wall slip during shearing.[11–13]

Currently, the extrusion flow simulations are based on rheological models without considering slip, which however alters the flow data of highly filled compounds substantially. Full understanding of a wall slippage together with reliable flow models[14–16] and accounting for a pressure-dependent

[1]Centre of Polymer Systems, University Institute, Tomas Bata University in Zlin, Zlin, Czech Republic.
[2]Department of Production Engineering, Faculty of Technology, Tomas Bata University in Zlin, Zlin, Czech Republic.
[3]Indo MIM Pvt. Ltd., Bangalore, India.
[i]ORCID ID (https://orcid.org/0000-0002-6368-7896).

viscosity[17] would lead to precise simulations of a forming process (flow patterns during extrusion or injection molding as a function of pressure, temperature, and velocity) and avoiding classical time-consuming and costly trial-and-error experiments to set up processing conditions of the forming steps.

As found out by LeBlanc et al.[18] and Saidy et al.,[19] technological limitations of additive manufacturing arise mostly from unstable behavior of polymer binders. Wall slip has been recently linked to the extrudate distortions and overall extrusion defects observed in the capillary flow of highly viscous polymer systems, and it may limit adhesive strength of deposited filaments.[20] The presence of domains deformed along the angular direction of the extrudate may also be attributed to slip.[21] Vadodaria et al.[22] reported heterogeneous flow profiles across the measurement gap due to the discontinuous shear gradient across the measurement gap as a consequence of wall slip during measurement of cellulose systems widely used in 3D printing.

Wall slip effect on the extrudability and windability of filaments was recently confirmed by Hasib et al.[23] for feedstocks based on polylactic acid and Ni–Cu powders. Furthermore, the relation between yield stress and shear stress at the wall affected by wall slip was investigated in some studies[24–26]; the wall shear stress higher than the yield stress potentially leads to the phase separation and inhomogeneous print quality. In contrast, wall slip phenomenon might prevent clogging of the nozzle,[27] but binder rich areas at filament walls might not ensure quality of sintered parts.

In general, the wall slip theory of highly filled polymers[28] assumes that upon shearing a narrow polymer layer of low viscosity with a typical thickness of 0.1–1 μm is created near the wall, and solid particles migrate to the middle of the flow channel. This means that a homogenous distribution of a powder within a polymer binder is disrupted,[29–31] and compounds show a phase separation that has a detrimental effect on final sintered structures. Delime and Moan[32] assumed that the migration of solid particles is initiated by a failure of Brownian movement near walls, which is supported by shear rate gradients, which promote particle collisions.[30,32] This theory was experimentally confirmed by Lam et al.[33] for the particles ranging from 20 to100 μm.

The magnitude of the wall slip depends significantly on a roughness and chemical nature of a processing tool used. For example, stainless steel was found to be more prone to a wall slip than aluminum,[34] and the rough surfaces, where solid particles can move into a groove, may suppress the formation of a low molecular layer on channel walls and reduce slip.[35]

During testing of metal powders (316L, 17–4PH) in a catalytic binder system as well as ZrO_2 feedstocks the same trend was obtained with the viscosity strongly affected by the surface roughness (smooth surfaces led to the lower viscosity and higher wall slip velocity).[36] These results corresponded to those of pure polymers[34] as well as suspensions containing polymer matrix poly(butadiene–acrylonitrile–acrylic acid) filled with glass spheres (particles mean size 35 and 85 μm)[37] and poly(methyl methacrylate) solid spheres (121 μm) in hydroxyl-terminated polybutadiene.[38] So far, smooth flow channel walls and small channels were found to be the most significant factors causing wall slip.[30,39]

The metal powder compounds for MEX and PIM contain particles of broad particle size distributions (typically from 0.1 to 20 μm) and various shapes—small particles ensure faster sintering but slow down debinding, spherical shape improves flow but irregular enhances a component strength before sintering, wide size distribution lowers sintering shrinkage but slows down debinding, and promotes quality issues and inhomogeneities in a structure.[40,41]

In this article, the materials investigated were selected based on our previous studies of the effect of shape and size of steel powders on the overall processing performance of highly filled compounds, where it was found that coarser (mean size of 11 and 20 μm) gas (GA) atomized particles are required to lower mixing torque, obtain higher critical solid loading and lower viscosity due to the lower friction between particles. However, in case of water (WA) atomized powders, fine powders (mean size of 3 and 8 μm) show a better performance.[42] Furthermore, it was found out that only a slight variation in particle size distribution fractions significantly influences the quality of the green components and dimensional tolerances of the complex-shaped components.[43]

The effect of powder shape and size is addressed in this study through a thorough analysis of the wall slip with the help of Mooney[44] method of determination of slip velocity. To our best knowledge, this important aspect of MEX has not been reported heretofore. Successful MEX requires tailored particle size distribution at multiple scales—particle sizes capable of retaining compound cohesion to enable flow as well as provide enough yield stress to the mixture, shape stability, and green strength. Size distribution is also a contributing factor to liquid phase migration under extrusion pressure, leading to flow-induced heterogeneities in the printed structure.[25] If one considers that the thickness of the polymer layer created near the channel wall during slippage is proportional to the square root of the wall slip velocity,[45,46] it may form in the critical places of the proceeded specimen, and thus cause the collapse of its surface or even bulk during sintering.[47]

Moreover, as demonstrated in our recent article,[48] the application of flat or conical dies might affect the rheological data obtained for highly concentrated particulate systems. Thus, the possible influence of an entrance angle of capillary dies on the evaluation of wall slip will be considered in this study as well.

Experimental

Materials

GA and WA atomized stainless steel powders 17–4PH with D_{50} of about 3 and 20 μm were provided by IndoMIM Pvt. Ltd., India. The particle size distribution of powders (Table 1) was measured using laser diffraction method (Malvern Mastersizer 3000).

TABLE 1. PARTICLE SIZE DISTRIBUTION OF POWDERS

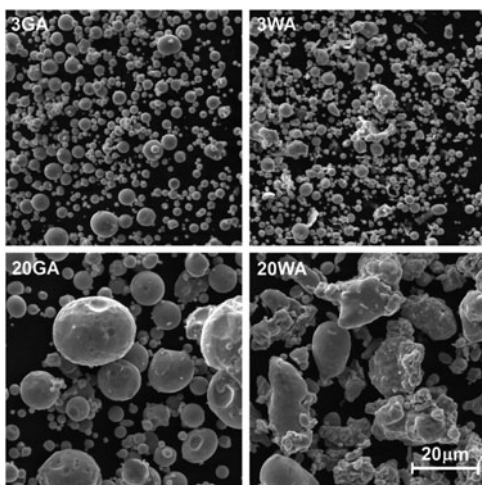| Powder	D_{10} (μm)	D_{50} (μm)	D_{90} (μm)
3GA	1.7	2.9	4.8
3WA	1.5	3.0	6.1
20GA	6.7	21.9	49.2
20WA	7.2	23.8	57.0

GA, gas; WA, water.

FIG. 1. SEM of GA and WA atomized 17-4PH stainless steel powders. GA, gas; SEM, scanning electron microscope; WA, water.

The morphology of powders was observed with a scanning electron microscope (VEGA II, TESCAN) as shown Figure 1.

Feedstock preparation

Feedstocks were prepared using low-density polyethylene, ethylene vinyl acetate, and paraffin wax-based binder system developed by Hausnerova et al.[49] (Table 2). The values of melting temperatures and densities were taken from the datasheets of the particular suppliers. Powder and binder were compounded using Z-blade laboratory mixer MZ05 (Winkworth) at 140°C for 20 min and a blade speed of 25–30 RPM. An optimum solid loading of 55 vol. % powder was set as 4 vol. % lower than the critical solid loading value of 20WA (lowest from the materials investigated, Table 3). The critical solid loading of powders was measured using the mixing torque method by plastometer Brabender W50; the detailed description of the method can be found in our previous study.[42]

Wall slip analysis

Wall slip was evaluated using a capillary rheometer (Göettfert 50; Göttfert Werkstoff-Prüfmaschinen GmbH, Buchen, Germany). Mooney rheological analysis was performed on the conical (90°) and flat (180°) dies (Fig. 2) with

TABLE 2. RELEVANT PHYSICAL PROPERTIES OF BINDER POLYMERS

Polymer	Content (wt. %)	Density (g/cm³)	Melt temperature (°C)
LDPE[a]	53	0.914	102
EVA[b]	26	0.948	67
PW[c]	21	0.900	50

[a]ExxonMobil™ LDPE LD 650 Low Density Polyethylene Resin.
[b]ExxonMobil Escorene™ Ultra UL 40028CC Ethylene Vinyl Acetate Copolymer Resin.
[c]FAGRON Paraffinum Solidum.

TABLE 3. CRITICAL SOLID LOADING (VOL. %)

3 μm		20 μm	
Gas	Water	Gas	Water
61	62	65	59

length to diameter (L/D) ratios of 5/0.5, 7/0.7, and 10/1 at 150°C. The diameter of the dies was kept between 0.5 and 1 mm, because the larger capillary diameter than 1 mm might result in an unstable pressure,[48] and smaller diameters than 0.5 caused blocking of the dies. Pressures used were 35, 42, 50, 59, 69, 88, 109, 137, 185, and 240 bars to cover uniformly as wide range of pressures as possible. Mooney method is based on changing the surface-to-volume ratio of the capillary dies, that is, changing length L and radius R of the dies, whereas their ratio is kept constant. In a circular die an apparent wall shear rate $\dot{\gamma}_a$ and an apparent wall shear stress τ_a are determined from the relations:

$$\dot{\gamma}_a = \frac{4\dot{Q}}{\pi R^3}; \tau_a = \frac{\Delta p R}{2L}, \qquad (1)$$

where $\dot{Q}$ is the volumetric flow rate and Δp is the measured pressure drop.

Consequently, a true average velocity is given by the difference between an average v_{av} ($=\dot{Q}/\pi R^2$) and a slip v_{slip} velocities:

$$v_{true} = v_{av} - v_{slip}. \qquad (2)$$

Multiplying this relation by 4/R and using the relation (1) a dependence of a corrected apparent shear rate on a measured apparent shear rate and wall slip velocity is obtained:

$$\dot{\gamma}_{a,\ slip-corrected} = \dot{\gamma}_a - \frac{4v_{slip}}{R}. \qquad (3)$$

The measurements at constant shear stress (pressure) have to be made with capillaries of different diameters, but the same L/D ratio. The obtained apparent shear rate values ($\dot{\gamma}_a$) are plotted into the graph as the function of the reciprocal radius of the capillary die (Fig. 3). The values of each measured pressure are then interpolated by linear regression, which is described by Equation 3. Finally, wall slip velocities are calculated from the slopes (a slope is equal to $4v_{slip}$) of these linear fittings, and expressed as a function of the shear stress in the graph.

Results and Discussion

According to the apparent data, all tested feedstocks exhibit a pseudoplastic behavior at 150°C as can be seen in Figure 4 for flat capillary dies. The data obtained for conical capillary dies were similar (Supplementary Fig. S1). Three of the tested materials (3GA, 3WA, and 20GA) show similarly low apparent viscosity values in the range of 80–600 Pa s, which may indicate their slippage at the wall. The apparent viscosity of irregular 20WA compound is about a decade higher than the values of other compounds. This is attributed
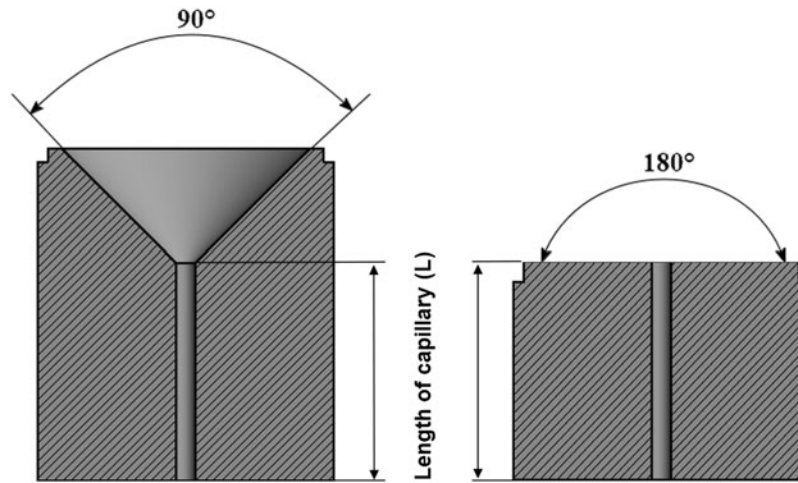
FIG. 2.   Schematic representation of conical (90°) and flat (180°) testing capillaries.

to the irregular shape of particles, because higher friction of the irregular particles[50] might overcome the effect of a size in case of coarse particles.[42] Partly, there is also a possible effect of the overall lowest critical solid loading of this compound (59 vol. %) in comparison with other compounds tested (Table 3).

As can be seen in Figure 5, representing the Mooney plots for the flat capillary dies (for conical capillary dies see Supplementary Fig. S2), an increasing tendency toward the wall slip with increasing shear stress/pressure is obvious from the slopes of the fitting lines of Mooney plots. The linear fitting lines with coefficients of determination higher than 0.995 were obtained.

The calculated values of the wall slip velocity (Fig. 6) clearly show the influence of the size and the shape on the wall slip phenomenon, which consequently governs the overall flow performance of the materials during processing. According to our best knowledge there is no report heretofore on the effect of the shape of the metal particles on the wall slip. The feedstocks containing spherical (GA) particles exhibit higher wall slip velocities than irregularly (WA) shaped powders of the comparative sizes, suggesting that spherical particles are more prone to wall slip. It is known that the slip of highly concentrated materials is connected to the separation of powder and binder—particles migrate to the middle of the flow channel due to the shear rate gradients during processing, and the low viscosity polymer layer forms near the die wall.[11,51–53]
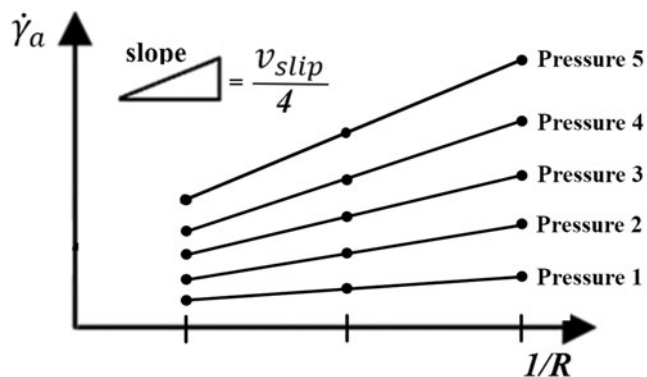

FIG. 3.   Schematic of a wall slip velocity evaluation using Mooney analysis.

In this perspective, the spherical particles seem to be more sensitive to shear rate gradients; as they do not have any preferential orientation dimension (aspect ratio is near 1), they can more easily start to rotate upon shearing as described by Thornagel[54] and move to the center of the die allowing for the formation of the polymer slip layer. This, as mentioned in Introduction, may lead to an anisotropic shrinkage and other associated defects inside final sintered products.[2,55] In contrast, WA atomized particles having a flake-like shape tend to orient with the flow front and sustain shearing without losing the uniform distribution within the polymer medium.

If the effect of particle sizes is considered, the data depicted in Figure 6 confirm the findings obtained by Sanetrnik et al.[36] and Chin et al.,[56] where the larger particles were more prone to the wall slip than smaller particles, because fine particles more easily fill the space near the wall, and thus prevent the formation of the polymer layer.

Based on these results, processing of small and irregular particles seems to be more advantageous in terms of a wall slip. Furthermore, it is in accordance with the effect of small particles in reducing powder/binder separation and improving a product homogeneity reported in.[51,57] At this point it should be pointed out that highly concentrated compounds for PIM and MEX undergo the changes of the particle shape and size during processing as recently reported by Bek et al.,[58] which might be also favorable in reducing a slip.

As can be further noted from Figure 6, the flat dies, which are commonly used in a vast majority of current studies,[28,59] result in the different wall slip velocities than the values obtained with the conical dies. Liang[60] and Ardakani et al.[61] tested changes in a pressure drop for different capillary entrance angles during extrusion, and showed that the geometrical arrangement of capillary dies of rheometers may significantly affect rheological data; in their case, the shear rate increased with the capillary entrance angle under the constant pressure. Furthermore, Sanetrnik et al.[48] reported that capillary entrance angles may affect the accuracy of the flow data, and consequently flow simulations carried out to optimize processing. The application of the conical dies was validated as more beneficial for highly filled materials as they do not cause rapid changes in shear rates.

As can be seen from Figure 7, the wall slip velocities of all tested materials at higher shear stresses, which are usually
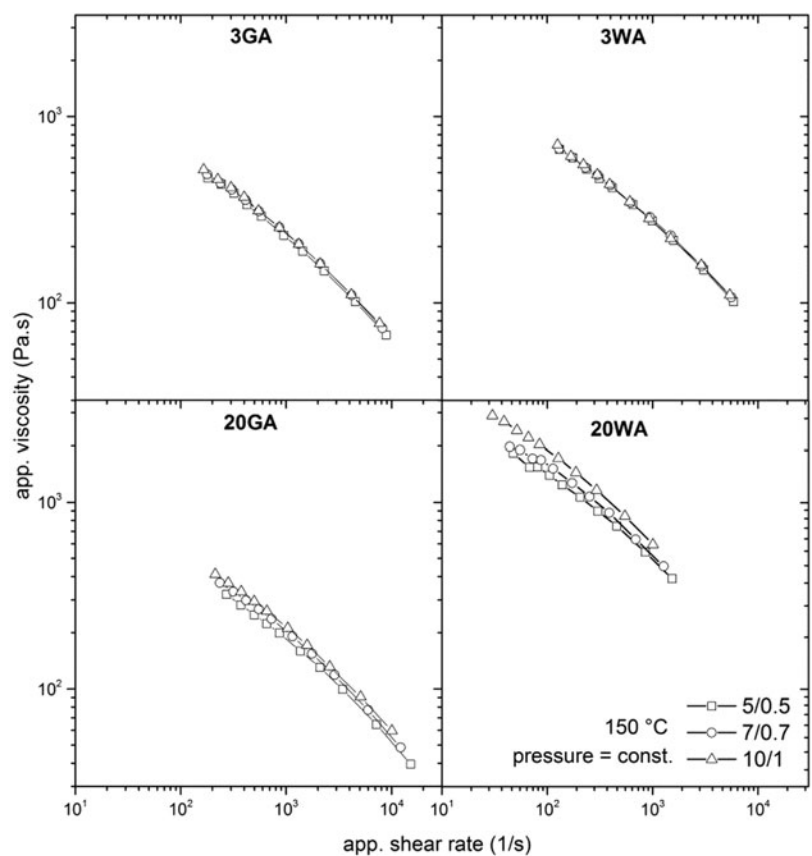
FIG. 4.   Apparent viscosity as a function of apparent shear rate of 17-4PH feedstocks varying in size and shape obtained with flat capillary dies (entrance angle 180°).
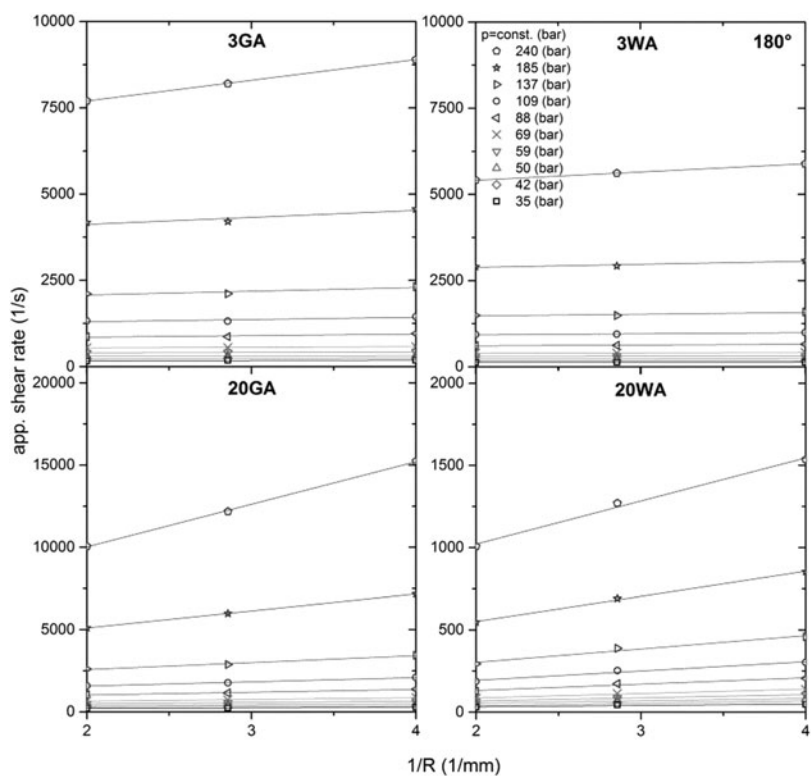

FIG. 5.   Mooney diagrams of 17-4PH feedstocks varying in size and shape obtained with flat capillary dies (entrance angle 180°).
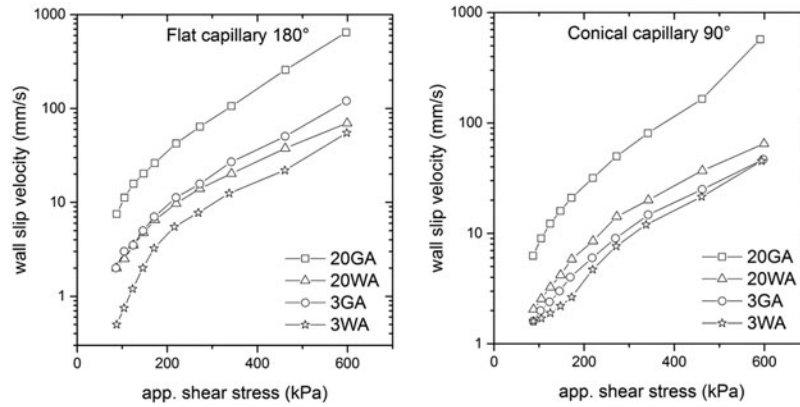
5

FIG. 6.　Wall slip velocities of 17-4PH feedstocks affected with powder shape and size obtained at various shear stresses on flat (entrance angle 180°) and conical (entrance angle 90°) dies.

used in MEX as well PIM, obtained with the conical capillaries are lower than those obtained with the flat dies, whereas at lower shear stresses the differences are rather negligible. Especially, fine and regular particles (3GA) react sensitively to the change of the entrance to the capillary die—at shear stresses about 600 kPa the wall slip velocity was reduced up to 60% with a conical dies. Based on these results and previous research[29–31,62] it is assumed that highly pronounced slip of small and regular particles measured on flat capillary dies may be attributed to their higher sensitivity to the
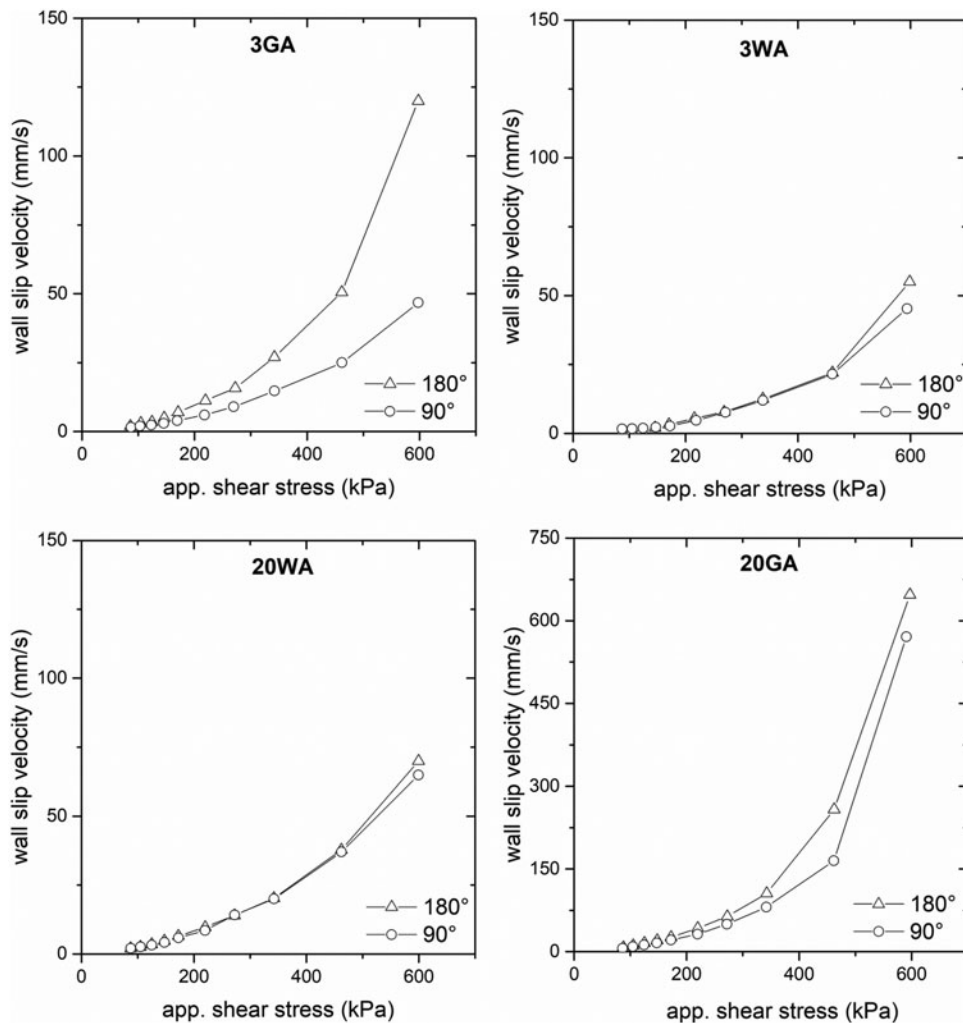

FIG. 7.　Influence of capillary die entrance angle on wall slip velocity of 17-4PH feedstocks varying in size and shape (note different magnitudes of y-axes).

changes of shear rate gradients at the entrance to the capillary, which are increasing function of entrance angle. This result is also supported with a flow pattern proposed for highly filled compounds by Thornagel.[54] As regular and fine particles are assumed to be more free to rotate and leave areas with higher shear rate gradients, they are more sensitive to the shear rate changes during flow in a capillary as well.

According to these findings, utilizing lower print/injection speeds, conical dies, loadings closer to a critical value, and generally ensuring more viscous melts may help to reduce wall slip, and consequently powder/binder separation resulting in defects on sintered parts.

Conclusion

Highly filled (55 vol. %) MEX and PIM compounds based on metal powders varying in shape and size are sensitive to wall slip as a crucial processability parameter whose neglecting results in an inaccurate rheological data. The effect of the shape of the particles not investigated heretofore was found to be more pronounced than the effect of the size. Spherical (GA atomized) and large (20μm) particles appear to be more sensitive to wall slip than irregular (WA atomized) and small (3μm). In addition, the geometry of the testing tool (entrance angle of a capillary die) might significantly affect determination of wall slip, and thus should be accounted for especially in the case of small and regular particles.

Author Disclosure Statement

No competing financial interests exist.

Funding Information

Supplementary Material

Supplementary Figure S1
Supplementary Figure S2

References

1. Shang F, Wang Z, Chen X, et al. UNS S32707 hyper-duplex stainless steel processed by powder injection molding and supersolidus liquid-phase sintering in nitrogen sintering atmosphere. Vacuum 2021;184:109910.

2. Gonzalez-Gutierrez J, Cano S, Schuschnigg S, et al. Additive manufacturing of metallic and ceramic components by the material extrusion of highly-filled polymers: A review and future perspectives. Materials 2018;11:840.

3. Kukla C, Gonzalez-Gutierrez J, Cano S, et al. Fused filament fabrication (FFF) of PIM feedstocks. In: VI Congreso Nacional de Pulvimetalurgia y I Congreso Iberoamericano de Pulvimetalurgia. 7–9 June 2017. Ciudad Real. Spain. 2017. 1–6.

4. Sa'ude N, Masood SH, Nikzad M, et al. Dynamic mechanical properties of copper-ABS composites for FDM feedstock. Int J Eng Res Appl 2013;3:1257–1263.

5. Masood SH, Song WQ. Development of new metal/polymer materials for rapid tooling using Fused deposition modelling. Mater Des 2004;25:587–594.

6. Giberti H, Strano M, Annoni M. An innovative machine for Fused Deposition Modeling of metals and advanced ceramics. In: International Conference on Nano and Materials Science. 1–2 April 2016. Prague. Czech Republic. MATEC Web of Conferences 2016;43:03003.

7. Rane K, Landro LD, Strano M. Processability of SS316L powder—Binder mixtures for vertical extrusion and deposition on table tests. Powder Technol 2019;345:553–562.

8. Mannschatz A, Hohn S, Moritz T. Powder-binder separation in injection moulded green parts. J Eur Ceram Soc 2010;30:2827–2832.

9. Heaney DF. Handbook of Metal Injection Molding. Cambridge, UK: Woodhead Publishing, 2012.

10. Huang B, Liang S, Qu X. The rheology of metal injection molding. J Mater Process Technol 2003;137:132–137.

11. Suri P, German RM, De Souza JP, et al. Numerical analysis of filling stage during powder injection moulding: Effects of feedstock rheology and mixing conditions. Powder Metall 2013;47:137–143.

12. Park SJ, Ahn S, Kang TG, et al. A review of computer simulations in powder injection molding. Int J Powder Metall 2010;46:37–46.

13. Hwang CJ, Kwon TH. A full 3D finite element analysis of the powder injection molding filling process including slip phenomena. Polym Eng Sci 2004;42:33–50.

14. Hausnerova B, Marcanikova L, Filip P, et al. Optimization of powder injection molding of feedstock based on aluminum oxide and multicomponent water-soluble polymer binder. Polym Eng Sci 2011;51:1376–1382.

15. Claudel D, Sahli M, Barriere T, et al. Influence of particle-size distribution and temperature on the rheological properties of highly concentrated Inconel feedstock alloy 718. Powder Technol 2017;322:273–289.

16. Filip P, Hausnerova B, Hnatkova E. Continuous rheological description of highly filled polymer melts for material extrusion. Appl Mater Today 2020;20:100754.

17. Hausnerova B, Sedlacek T, Slezak R, et al. Pressure-dependent viscosity of powder injection moulding compounds. Rheol Acta 2006;45:290–296.

18. LeBlanc KJ, Niemi SR, Bennett AI, et al. Stability of high speed 3D printing in liquid-like solids. ACS Biomater Sci Eng 2016;2:1796–1799.

19. Saidy NT, Shabab T, Bas O, et al. Melt electrowriting of complex 3D anatomically relevant scaffolds. Front Bioeng Biotechnol 2020;8:793.

20. Mackay ME. The importance of rheological behavior in the additive manufacturing technique material extrusion. J Rheol 2018;62:1549.

21. Maciel A, Salas V, Soltero JFA, et al. On the wall slip of polymer blends. J Polym Sci B Polym Phys 2002;40:303–316.

22. Vadodaria SS, Onyianta AJ, Sun D. High-shear rate rheometry of micro-nanofibrillated cellulose (CMF/CNF) suspensions using rotational rheometer. Cellulose 2018;25:5535–5552.

23. Hasib AG, Niauzorau S, Xu W, *et al.* Rheology scaling of spherical metal powders dispersed in thermoplastics and its correlation to the extrudability of filaments for 3D printing. Addit Manuf 2021;41:101967.

24. Bryan MP, Rough SL, Wilson DI. Measurement of the wall slip behaviour of a solid granular soap in ram extrusion. Powder Technol 2018;323:76–85.

25. Nair SAO, Alghamdi H, Arora A, *et al.* Linking fresh paste microstructure, rheology and extrusion characteristics of cementitious binders for 3D printing. J Am Ceram Soc 2019;102:3951–3964.

26. Alghamdi H, Nair SAO, Neithalath N. Insights into material design, extrusion rheology, and properties of 3D-printable alkali-activated fly ash-based binders. Mater Des 2019;167:107634.

27. Kotsilkova R, Tabakova S, Ivanova R. Effect of graphene nanoplatelets and multiwalled carbon nanotubes on the viscous and viscoelastic properties and printability of polylactide nanocomposites. Mech Time Depend Mater 2021, DOI: 10.1007/s11043-021-09503-2.

28. Lam YC, Wang ZY, Chen X, *et al.* Wall slip of concentrated suspension melts in capillary flows. Powder Technol 2007;177:162–169.

29. Denn MM. Extrusion instabilities and wall slip. Ann Rev Fluid Mech 2001;33:265–287.

30. Barnes HA. A review of the slip (wall depletion) of polymer solutions, emulsions and particle suspensions in viscometers: Its cause, character, and cure. J Non-Newton Fluid Mech 1995;56:221–251.

31. Bryan MP, Rough SL, Wilson DI. Investigation of static zones and wall slip through sequential ram extrusion of contrasting micro-crystalline cellulose-based pastes. J Non-Newton Fluid Mech 2015;220:57–68.

32. Delime A, Moan M. Lateral migrations of solid spheres in tube flow. Rheol Acta 1991;30:131–139.

33. Lam YC, Chen X, Tan KW, *et al.* Numerical investigation of particle migration in poiseuille flow of composite system. Compos Sci Technol 2004;64:1001–1010.

34. Chen Y, Kalyon M, Bayramli E. Effects of surface roughness and the chemical structure of materials of construction on wall slip behavior of linear low density polyethylene in capillary flow. J Appl Polym Sci 1993;50:1169–1177.

35. Medhi BJ, Kumar AA, Singh A. Apparent wall slip velocity measurements in free surface flow of concentrated suspensions. Int J Multiph Flow 2011;37:609–619.

36. Sanetrnik D, Hausnerova B, Pata V. Online rheometry investigation of flow/slip behavior of powder injection molding feedstocks. Polymers 2019;11:432.

37. Aral BK, Kalyon DM. Effects of temperature and surface roughness on time-dependent development of wall slip in steady torsional flow of concentrated suspensions. J Rheol 1998;38:957–972.

38. Gulmus SA, Yilmazer U. Effect of the surface roughness and construction material on wall slip in the flow of concentrated suspensions. J Appl Polym Sci 2006;103:3341–3347.

39. Jeong M, Kim Y, Zhou W, *et al.* Effects of surface wettability, roughness and moving wall velocity on the Couette flow in nano-channel using multi-scale hybrid method. Comput Fluids 2017;147:1–11.

40. German RM. Metal Injection Molding. Princeton, NJ: Metal Powder Industries Federation, 2011.

41. Cano S, Gonzalez-Gutierrez J, Sapkota J, *et al.* Additive manufacturing of zirconia parts by fused filament fabrication and solvent debinding: Selection of binder formulation. Additive Manuf 2019;26:117–128.

42. Hausnerova B, Mukund BN, Sanetrnik D. Rheological properties of gas and water atomized 17–4PH stainless steel MIM feedstocks: Effect of powder shape and size. Powder Technol 2017;312:152–158.

43. Mukund BN, Hausnerova B. Variation in particle size fraction to optimize metal injection molding of water atomized 17–4PH stainless steel feedstocks. Powder Technol 2020;368:130–136.

44. Mooney M. Explicit formulas for slip and fluidity. J Rheol 1931;2:210–222.

45. Meeker SP, Bonnecaze RT, Cloitre M. Slip and flow in pastes of soft particles: Direct observation and rheology. J Rheol 2004;48:1295–1320.

46. Aktas S, Kalyon DM, Marin-Santibanez BM, *et al.* Shear viscosity and wall slip behavior of a viscoplastic hydrogel. J Rheol 2014;58:513–535.

47. Hwang KS. Common defects in metal injection molding (MIM). In: Heaney DF. (ed.) Handbook of Metal Injection Molding. Sawston, UK: Woodhead Publishing, 2012; pp.235–253.

48. Sanetrnik D, Hausnerova B, Filip P, *et al.* Influence of capillary die geometry on wall slip of highly filled powder injection molding compounds. Powder Technol 2018;325:615–619.

49. Hausnerova B, Saha P, Kubat J, *et al.* Rheological behaviour of hard-metal carbide powder suspensions at high shear rates. J Polym Eng 2000;20:237–266.

50. Yunn HS, Muhamad N, Sulong AB, *et al.* Critical solid loading and rheological study of WC-10%Co. Appl Mech Mater 2011;52–54:97–102.

51. Fang W, He XB, Zhang RJ, *et al.* Effects of particle characteristics on homogeneity of green bodies in powder injection moulding. Powder Metall 2014;57:274–282.

52. Supati R, Loh NH, Khor KA, *et al.* Mixing and characterization of feedstock for powder injection molding. Mater Lett 2000;46:109–114.

53. Kate KH, Enneti RK, Park SJ, *et al.* Predicting powder-polymer mixture properties for PIM design. Crit Rev Solid State Mat 2014;39:197–214.

54. Thornagel M. MIM-simulation: A virtual study on phase separation. In: International Powder Metallurgy Congress & Exhibition. 2009. Copenhagen. Denmark: European Powder Metallurgy Association, 2009; pp.135–140.

55. Gonzalez-Gutierrez J, Stringari G, Emri I. Powder injection molding of metal and ceramic parts. In: Wang J. (ed.) Some Critical Issues for Injection Molding. IntechOpen, UK, 2012; pp.65–86.

56. Chin RJ, Lai SH, Ibrahim S, *et al.* Factors affect wall slip: Particle size, concentration and temperature. Appl Rheol 2018;28:15775.

57. Trad MAB, Demers V, Dufresne L. Effect of powder shape and size on rheological, thermal, and segregation properties of low-pressure powder injection molding feedstocks. J Mater Eng Perform 2019;28:5551–5562.

58. Bek M, Gonzalez-Gutierrez J, Kukla C, *et al.* Rheological behaviour of highly filled materials for injection moulding and additive manufacturing: Effect of particle material and loading. Appl Sci 2020;10:7993.

59. Wilms P, Wieringa J, Blijdenstein T, *et al.* Wall slip of highly concentrated non-Brownian suspensions in pressure

driven flows: A geometrical dependency put into a non-Newtonian perspective. J Non-Newton Fluid Mech 2020; 282:104336.

60. Liang JZ. Influence of die angles on pressure drop during extrusion of rubber compound. J Appl Polym Sci 2001; 80:1150–1154.

61. Ardakani HA, Mitsoulis E, Hatzikiriakos SG. Thixotropic flow of toothpaste through extrusion dies. J Non-Newton Fluid Mech 2011;166:1262–1271.

62. Soltani F, Yilmazer U. Slip velocity and slip layer thickness in flow of concentration suspensions. J Appl Polym Sci 1998;70:515–522.

Address correspondence to:
Berenika Hausnerova
Department of Production Engineering
Faculty of Technology
Tomas Bata University in Zlin
nam. T.G. Masaryka 5555
Zlin 760 01
Czech Republic

E-mail: hausnerova@utb.cz